Astron. Astrophys. 293, 381–395 (1995)

ASTRONOMY AND ASTROPHYSICS

The evolution of galactic carbon stars

M.A.T. Groenewegen[1,2], L.B. van den Hoek[1], and T. de Jong[1,3]

[1] Astronomical Institute 'Anton Pannekoek', Kruislaan 403, NL-1098 SJ Amsterdam, The Netherlands
[2] present address: Institut d'Astrophysique de Paris, CNRS, 98 bis Bd. Arago, F-75014 Paris, France
[3] SRON, Laboratory for Space Research, P. O. Box 800, NL-9700 AV Groningen, The Netherlands

Received 21 February 1994 / Accepted 5 July 1994

Abstract. Based on a comparison of observations with new synthetic AGB evolution calculations we propose a revised evolutionary scenario for carbon stars in the solar neighbourhood. From observations we derive that the lowest initial mass from which carbon stars form is about 1.5 $M_\odot$. This constraint combined with four other constraints (the observed initial-final mass relation, the birth rate of carbon stars, the observed abundance ratios in planetary nebulae (PNe) and the number ratios C/M and S/C of AGB stars) are used to derive the following parameters for the synthetic AGB evolution model. Third dredge-up occurs for core masses above 0.58 $M_\odot$ and the dredge-up efficiency is $\lambda = 0.75$. We consider a Reimers mass loss law (with a scaling factor η_{AGB}) and the mass loss rate law recently proposed by Blöcker & Schönberner (1993; with a scaling factor η_{BS}). We find $\eta_{AGB} = 4$ and $\eta_{BS} = 0.08$. Both models fit the observations equally well.

The model predicts that stars in the range $1.5\ M_\odot \lesssim M \lesssim 1.6\ M_\odot$ become carbon stars at their last thermal pulse (TP) on the AGB and live only a few 10^4 yr as carbon stars. More massive stars experience additional TPs as carbon stars (up to about 25 for a 3 $M_\odot$ star) and live up to 10^6 yr. For $M \gtrsim 4\ M_\odot$ hot-bottom burning prevents the formation of carbon stars. For $M \lesssim 2\ M_\odot$, M-stars skip the S-star phase when they become carbon stars. The average lifetime of the carbon star phase is $\sim 3\ 10^5$ yr.

The carbon stars for which C/O ratios have been derived in the literature (with values $\lesssim 1.5$) are predominantly optical carbon stars with a 60 μm excess. Yet, disk PNe are known with C/O ratios up to about 4. We predict that carbon stars with C/O ratios $\gtrsim 1.5$ are to be found among the infrared carbon stars. The model predicts that the probability that a carbon star has C/O $\gtrsim 1.5$ is about 30%, in reasonable agreement with the observed ratio of the surface density in the galactic plane of infrared carbon stars to all carbon stars. The infrared carbon stars are predicted to be (on average) more massive than the optical carbon stars.

The fact that carbon stars with C/O $\gtrsim 1.5$ apparently never reach the optical carbon star phase (with a detached shell) is probably due to differences in evolution. If indeed infrared carbon stars are on average more massive (i.e. have larger core masses) than optical carbon stars, the interpulse period is shorter, and the increase in luminosity during the TP is smaller (due to the larger envelope mass). Both effects will decrease the likelihood of a detached shell to occur. We predict that two-thirds of all detached shells around optical carbon stars are oxygen-rich.

Key words: stars: carbon – stars: evolution – stars: mass loss – stars: AGB – planetary nebulae: general

1. Introduction

The study of carbon stars has gained significant momentum by studying their infrared and molecular properties. A large number of carbon stars radiate predominantly in the near- and far-infrared and there are even carbon stars (the infrared carbon stars) with no or very faint optical counterparts.

Different samples of carbon stars, selected on the basis of infrared properties, were studied by Claussen et al. (1987), Thronson et al. (1987), Willems (1988a, b), Jura et al. (1989), Jura & Kleinmann (1989) and Groenewegen et al. (1992). It was recognised that many optical carbon stars have an excess at 60 μm (Willems 1988a). This raised questions on the evolution of carbon stars in general, and that in the IRAS color-color diagram in particular.

Willems & de Jong (1988) proposed a scenario for carbon star evolution related to the occurrence of thermal pulses. In this scenario, the oxygen-to-carbon transition causes the mass loss to drop and the oxygen-rich circumstellar shell to expand and dilute. This gives rise to the characteristic excess at 60 μm observed in many optical carbon stars. Willems & de Jong (1988), Chan & Kwok (1988) and Egan & Leung (1991) modelled the evolution in the IRAS color-color diagram of a carbon star with a detached shell. They assumed the detached shell to be geometrically thick, i.e. they assumed the detached shell to correspond to the mass loss in the phase of quiescent H-burning prior to

Send offprint requests to: M. Groenewegen at IAP address

the thermal pulse that turned the star into a carbon star. It has become clear that this picture needs revision. By mapping the circumstellar shell of S Sct (a carbon star with a 60 μm excess) in CO (Olofsson et al. 1992; Yamamura et al. 1993) and fitting the spectral energy distribution (Groenewegen & de Jong 1994a) it has been shown that this detached shell is geometrically thin. Double-peaked CO line profiles have been observed in two additional carbon stars with a 60 μm excess (Olofsson et al. 1990). Although photodissociation may also play a role, the width of the shells are consistent with the scenario that they correspond to a brief (about 10^3 yr) period of high mass loss due to the enhanced mass loss immediately following the thermal pulse rather than due to the oxygen-to-carbon transition as suggested by Willems & de Jong (1989). Therefore we expect that the occurrence of detached shells is a general phenomenon in thermal pulsing AGB stars. This has been confirmed recently by Zijlstra et al. (1992) who showed that there are also M- and S-stars with an excess at 60 μm.

Based on their models, Willems & de Jong and Chan & Kwok estimated that the timescale to make a loop through the IRAS color-color diagram is about 2 10^4 yr. Assuming a geometrically thin shell and taking into account the limited beam-size of the IRAS detectors, Groenewegen & de Jong (1994a) showed for S Sct that this timescale is probably overestimated by about 30%.

Groenewegen et al. (1992) extended the evolutionary scenario of Willems & de Jong to the infrared carbon stars. They derived space densities and lifetimes under the assumption that the sequence of optical carbon stars to infrared carbon stars is an evolutionary sequence and that carbon stars only make one loop through the IRAS color-color-diagram. A total carbon star lifetime of ~26 000 yr was estimated.

The validity of this short carbon star lifetime has been questioned by Zuckerman and co-workers who also argued that the detached shell around optical carbon stars should be carbon-rich rather than oxygen-rich (Claussen et al. 1987; Jura 1988; Zuckerman & Maddalena 1989; Zuckerman 1993; but see de Jong 1989).

In this paper we want to address several questions regarding the evolution of carbon stars on the AGB: (1) what is the initial mass range that can form carbon stars, (2) what is the lifetime of the carbon star phase, (3) how many thermal pulses do carbon stars make and does this result in as many loops through the IRAS color-color diagram, (4) are the detached shells around optical carbon stars oxygen-rich or carbon-rich, and (5) is the distribution of carbon stars in the IRAS color-color-diagram a sequence in time or in initial mass?

To answer these questions we combine existing literature data with new synthetic AGB calculations, which already proved to be successful in explaining the properties of carbon stars and the abundance ratios in planetary nebulae (PNe) in the LMC (Groenewegen & de Jong 1993a, 1994b, 1994c). In Sect. 2 the synthetic AGB evolution model is introduced and the constraints are discussed in Sect. 3. In Sect. 4 the results of the calculations are presented. In Sect. 5 the evolutionary scenario is presented and discussed.

2. The synthetic AGB evolution model

The synthetic evolution model is explained in detail in Groenewegen & de Jong (1993a, Paper I). It is based on recent evolutionary calculations for low- and intermediate-mass stars. Here only the most important features are outlined and some improvements to the previous model are discussed. The calculations in the present paper supersede the preliminary calculations for the Galaxy presented in Table 5 of Paper I.

In the model a population of stars is selected according to the probability that they presently are on the AGB. This probability depends on the initial mass function, the star formation rate and the duration of the AGB phase, as outlined in Paper I. With such an approach, average population properties (e.g. a luminosity function) can be calculated, using as input the evolution of individual stars.

AGB evolution starts at the first thermal pulse and ends when the envelope mass of the AGB star is reduced to $\sim 10^{-3}$ $M_\odot$. The changes in the abundances due to the first and second dredge-up, prior to the AGB phase, are taken into account. On the AGB, third dredge-up is assumed to occur for core masses above $M_c^{\rm min}$. For the LMC we derived $M_c^{\rm min} = 0.58$ $M_\odot$ (Paper I). At each thermal pulse an amount $\Delta M_{\rm dredge} = \lambda \Delta M_c$ is added to the envelope, where ΔM_c is the core mass growth during the preceding interpulse period and λ is the dredge-up efficiency. For the LMC we derived $\lambda = 0.75$ (Paper I). The composition of the material dredged-up is assumed to be: carbon (22%), oxygen (2%) and helium (76%) (Boothroyd & Sackmann 1988), independent of pulse number.

Prior to the AGB, stars lose mass on the main sequence, on the Red Giant Branch (RGB; only important for stars below ~2.2 $M_\odot$ which experience the helium core flash) and on the Early-AGB (E-AGB; important for massive stars). The total mass lost by stars with initial masses $\lesssim$2.2 $M_\odot$ preceding the AGB is taken from the models of Sweigart et al. (1990) scaled in such a way to give a mass loss of 0.22 $M_\odot$ for a 0.85 $M_\odot$ star ($\eta_{\rm RGB} = 0.86$ in the nomenclature of Sect. 2.6.1 of Paper I). In Paper I we used the evolutionary tracks of Maeder & Meynet (1989) to estimate the mass loss rate prior to the AGB for massive stars. With the new tracks of Schaller et al. (1992) and Schaerer et al. (1993) it is possible to include a metallicity dependence. Equation 21 in Paper I is replaced by:

$$\Delta M_{\rm EAGB} = $$

$$= \eta_{\rm EAGB}\ 0.116 \left(\frac{Z}{0.008}\right)^{0.61} \left(\frac{M}{7}\right)^{1.97\,(\frac{Z}{0.008})^{0.35}} M_\odot. \qquad (1)$$

where M is the initial mass of the star in $M_\odot$ and Z the metallicity. Schaller et al. (1992) find a mass loss rate at the start of the thermal-pulsing AGB of 6.1 10^{-8} and 3.1 10^{-7} $M_\odot$/yr for a 3 and a 5 $M_\odot$ solar-metallicity star. In order to smoothly fit the E-AGB mass loss rate to the AGB mass loss rate we have adopted $\eta_{\rm EAGB} = 3$. This particular choice does not affect any of our results since $\Delta M_{\rm EAGB}$ is always much smaller than the envelope mass at the start of the TP-AGB. Unfortunately, observationally determined mass loss rates of massive E-AGB stars are unavailable to estimate $\eta_{\rm EAGB}$.

In Paper I mass loss on the AGB was described by a Reimers (1975) law with a scaling factor $\eta_{\rm AGB}$. For the LMC we derived $\eta_{\rm AGB}$ = 5 in Paper I. In Paper III (Groenewegen & de Jong 1994c) we showed that with the mass loss rate law proposed by Blöcker & Schönberner (1993; BS) an equally good fit to the observational constraints in the LMC can be obtained. In Paper IV (Groenewegen & de Jong 1994d) we showed that with the latter mass loss rate the slope in the observed relation between the mass loss rate and pulsation period is reproduced. In the present paper both mass loss laws are considered. The Reimers mass loss law is:

$$\dot{M} = \eta_{\rm AGB}\ 4.0\ 10^{-13}\ \frac{L\,R}{M} \qquad {\rm M}_\odot/{\rm yr}. \qquad (2)$$

with L, R and M in solar units. The mass loss rate law proposed by BS is:

$$\dot{M} = \eta_{\rm BS}\ \left(4.8\ 10^{-9}\ \frac{L^{2.7}}{M^{2.1}}\right)\ \left(4.0\ 10^{-13}\ \frac{L\,R}{M}\right)\ {\rm M}_\odot/{\rm yr} \quad (3)$$

i.e. a Reimers law with an additional ($L^{2.7}/M^{2.1}$) dependence. We include a scaling factor $\eta_{\rm BS}$. BS derived this law by fitting the mass loss rates listed by Bowen (1988) for his standard model based on dynamical calculations for long-period variables. Direct comparison of Eqs. (2) and (3) shows that the mass loss rate adopted by BS is equivalent to high Reimers coefficients. For representative values of L = 3000 $L_\odot$, M = 1 $M_\odot$ or L = 20 000 $L_\odot$, M = 5 $M_\odot$ the equivalent value of $\eta_{\rm AGB}$ are 12 and 67, respectively. Repeating the analysis of Papers I and II (Groenewegen & de Jong 1994b) we found that all constraints in the LMC can be fitted with $\eta_{\rm BS}$ = 0.1 (Paper III).

A major improvement to the model is the use of main sequence abundances for individual elements. In Paper I (Sect. 2.9.1) we used an age-metallicity relation (AMR) for the sum of the heavy elements Z and assumed that the decomposition of Z in carbon, oxygen and nitrogen is constant in time and equal to the solar value. Furthermore, the main sequence helium abundance was estimated from the primordial helium value and a simple differential ratio $\Delta Y/\Delta Z$ = 2.5.

In the present paper we use AMRs for individual elements including H, He, C, N and O as well as the heavy element integrated metal-abundance Z presented by van den Hoek et al. (1994). Their AMRs are based on a chemical evolution model for the solar neighbourhood using up-to-date stellar evolution data including metallicity dependent stellar lifetimes, element yields and remnant masses. The adopted star formation history and slope of the initial mass function have been derived taking into account observational constraints to the abundance-abundance variations with age, the [Fe/H] and age distribution of main-sequence F and G dwarfs as well as constraints to the current space density and formation rate of several post main-sequence star populations. A stellar lower mass limit of 0.1 $M_\odot$ and the slope γ of the initial mass function: $dN/dm = m^{-\gamma}$ with γ = 2.45 were used. In this paper we adopt a preliminary set of self-consistent models of van den Hoek et al. with an exponentially decreasing Star Formation Rate (SFR) (see Fig. 1).

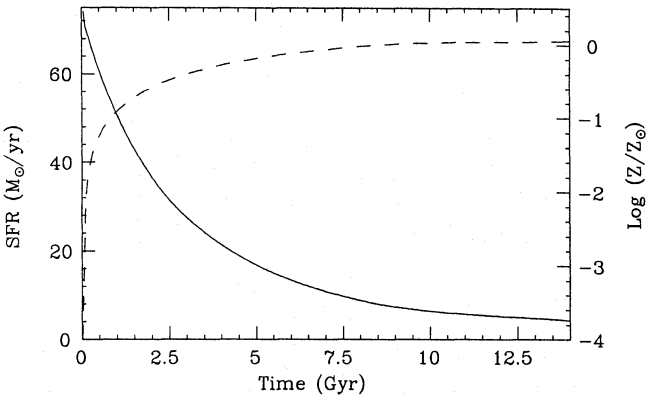

Fig. 1. The star formation rate (solid line; left-hand scale) and age-metallicity relation (dashed line, right-hand scale) adopted in this study for the solar neighbourhood (van den Hoek et al. 1994)

The tracks of Schaller et al. (1992) for Z = 0.02 have been used to calculate the total lifetime prior to the AGB. This lifetime is needed to estimate the metallicity of a star on the main sequence from the adopted AMR, and the SFR at the time of birth of a star. The age of the Galaxy is taken as 14 Gyr, indicating that the lower mass limit of stars that can reach the AGB is $M_{\rm lower}$ = 0.966 $M_\odot$ (from Schaller et al. 1992). The assumption of using tracks of constant metallicity to calculate the main-sequence lifetimes ignores the fact that stars of lower mass have lower metallicity and therefore live shorter. When this is taken into account $M_{\rm lower}$ is reduced to 0.82 $M_\odot$. This effect is discussed in Sect. 4.1. The upper mass limit is taken as $M_{\rm upper}$ = 8 $M_\odot$. More massive stars are assumed to evolve into supernovae.

3. The constraints

In this section we discuss five constraints to the synthetic evolution model. Four of these, the abundances of PNe, the birth rate of carbon stars, the number ratio of M-, S- and C-stars on the AGB, and the initial-final mass relation, are similar to those used for the LMC in Paper I, and are briefly discussed in Sect. 3.2. The fifth constraint, the mass range from which carbon and S-stars form, is discussed in detail below.

3.1. The mass range from which carbon stars and S-stars form

The most reliable information on the mass of C-stars (and S-stars) can be obtained from stars in binaries and open clusters. In a classical paper Gordon (1968) listed 10 candidates for binaries containing a carbon star and a less evolved star. Later work includes Barbaro & Dallaporta (1974), Olson & Richer (1975) who added some new candidates, Reimers & Grootte (1983) and Le Bertre (1990). Carbon stars in clusters are discussed by Gordon (1968), Barbaro & Dallaporta (1974), Bouchet & Thé (1983), Jørgensen (1988) and most recently by Eggen & Iben (1991).

In Table 1 all suspected binaries containing a carbon star with spectral type N (indicating the star is cool and therefore on

Table 1. Carbon stars in binaries and open clusters

C	IRAS-name	GCVS	S_{12} (Jy)	C_{21}	cluster name	age cluster (10^7 yr)	Sp. type companion	mass C-star ($M_\odot$)
471	03112−5730	TW Hor	94.0	-1.028	Hyades	60-150		1.9-2.5
789	04476+4335	HN Aur	2.78	-1.390	NGC 1664	1.0-3.2		3.5-5.1
853	05028+0106	W Ori	184.	-1.377	Pleiades	7		7
911	05185+3227	UV Aur	69.4	-1.317			B9V	$\gtrsim$3.5
1263	06217−2702		20.5	-1.293			A5V	$\gtrsim$2.2
1264	06225+1445	BL Ori	44.5	-1.258	Pleiades	7		7
1478	06528−4218	NP Pup	35.9	-1.120	Hyades	60-150		1.9-2.5
1549	07045−0728	RY Mon	58.8	-1.352			F3IV	$\gtrsim$1.5
1565	07057−1150	W CMa	39.0	-0.941			B2V	$\gtrsim$10.4
1859	07427−2816		1.47	-1.310	Haffner 14	16		4.3
1910	07487−3839	QT Pup	3.61	-1.280	NGC 2447	160-200		1.8-1.9
2063	08050−2939		4.61	-1.383	NGC 2533	16		4.3
2315	08408−4701	GV Vel	3.36	-1.183	NGC 2660	160-200		1.8-1.9
2685	09582−5958	SZ Car	24.7	-1.087	NGC 3114	10		5.1
3526	14417−6129		4.73	-1.411	Loden 1409	16		4.3
3875	17419−1838	SZ Sgr	18.6	-0.674			A7V	$\gtrsim$1.8
4111	18448+0523	DR Ser	16.0	-0.948			A6IV	$\gtrsim$2.1
4653	20028+2030	X Sge	16.8	-1.144			F2V	$\gtrsim$1.5
4716	20085+3547	RY Cyg	9.1	-1.325	NGC 6883	3.2-6.5		6.1-8.6
5570	22036+3315	RZ Peg	15.8	-0.874			F9V	$\gtrsim$1.2
5987	00020+4316	SU And	10.4	-1.219			F0V	$\gtrsim$1.7

the AGB) and a main sequence companion, and all N-type carbon stars which may be in open clusters are collected. Possible carbon stars with giant companions or companions of which the luminosity class is unknown or uncertain are not considered since no reliable masses can be estimated in these cases. In Table 1 the number in the Stephenson's catalog (1989), the IRAS-name[1], the variable star name, the 12 μm flux-density, the C_{21} color (defined as 2.5 $\log(S_{25}/S_{12})$), the cluster name, the age of the cluster, the spectral type of the companion and the estimated main sequence mass of the carbon star are listed. The spectral type of the companion is transformed into a mass using the spectral type-mass conversion of Straižys & Kuriliene (1981) and Schmidt-Kaler (1982). This method provides lower limits to the main sequence masses of carbon stars. An uncertainty of one spectral sub-class corresponds to an uncertainty of $\sim$0.06 $M_\odot$ at spectral type F2V, and of $\sim$2 $M_\odot$ at B2V. For the carbon stars in clusters the mass of the carbon star is estimated using the turn-off age and the tracks of Schaller et al. (1992). From Table 1 we derive that carbon stars are formed from stars above 1.8 $M_\odot$ (from the cluster data), although the data on carbon stars in binaries allows masses of $\gtrsim$1.2 $M_\odot$ for carbon star formation. The upper mass limit is more uncertain but is at least 5 $M_\odot$ and possibly higher.

The information on S-stars in binaries and clusters is scarce (see Scalo & Miller 1979). An additional complication is that S-stars are observed with and without the radioactive s-process element technetium (Tc). Only S-stars with Tc are believed to be on the AGB (see Groenewegen 1993; Jorissen et al. 1993). The S-stars with Tc in binaries are π Gru and the lithium-rich star T Sgr. The former has a G0V companion implying an initial mass for π Gru of $\gtrsim$1.1 $M_\odot$. On the other hand, π Gru is normally associated with the Hyades implying a mass of 1.9-2.5 $M_\odot$ (see Table 1). The star T Sgr has an F3IV companion implying an initial mass of $\gtrsim$1.5 $M_\odot$. S-stars possibly in clusters are the lithium-rich star TT9 (in N 3372, M $\gtrsim$10 $M_\odot$, no data on Tc), TT10 (in N 3372, M $\gtrsim$10 $M_\odot$, no data on Tc), TT12 (in N 3572b, M $\gtrsim$10 $M_\odot$, no data on Tc) and R And (in the Wolf 630 group, M $\approx$ 1.7 $M_\odot$, contains Tc).

Additional information about the typical mass of S-stars and C-stars comes from kinematical data and from some binaries containing a White Dwarf (WD).

Dean (1976) finds that the majority of carbon stars kinematically behave like F5 stars, although his Fig. 4 suggests that the spectral type is closer to F3, corresponding to a mass of about 1.5 $M_\odot$.

The S-stars without technetium, the barium-stars and the CH-stars appear to be in binary systems which consist of a WD and a star with enhanced (relative to normal giants) s-process elements and C/O ratio. These chemical peculiarities are believed to be due to a previous phase of mass transfer when the WD was on the AGB (see e.g. Jorissen & Mayor 1992; Groenewegen 1993; Jorissen et al. 1993). The presence of such systems places a lower limit to the mass at which third dredge-up occurs.

The mass function ($Q \equiv M_{\rm WD}^3/(M+M_{\rm WD})^2$) of the barium- and the S(no-Tc) stars is Q = 0.04-0.05 (Jorissen & Mayor 1992). Since the WD must have a core mass high enough for

[1] All stars turned out to be detected by IRAS. This was not a selection criterion.

third dredge-up to have occurred on the AGB ($M_{\rm WD} \geq M_{\rm c}^{\rm min}$) and experienced some core-growth during its AGB evolution, this implies a lower limit to the current mass of the secondary of 1.4 $M_\odot$ (for $Q = 0.05$ and $M_{\rm WD} = 0.57$ $M_\odot$) and a probable mass of 1.5 $M_\odot$ (for $Q = 0.044$ and $M_{\rm WD} = 0.58$ $M_\odot$). Since the secondary is probably on the RGB now, its main sequence mass may have been a little higher (by a few 10^{-2} $M_\odot$) due to mass loss on the RGB. On the other hand, if mass transfer from the former AGB star was very effective (due to Roche-lobe overflow) the secondary may now be more massive than on the main sequence. Jorissen & Boffin (1992) argue, however, that a wind accretion model can explain the observed chemical peculiarities of Ba-stars.

Considering all observational evidence we conclude that the lowest initial mass at which third dredge-up produces S-stars and C-stars occurs close to 1.5 $M_\odot$ (within 0.1 $M_\odot$). This conclusion is derived for, and expected to hold only in, environments of roughly solar metallicities. For the LMC, with its lower metallicity, the formation of carbon stars occurs near 1.2 $M_\odot$ (see Paper I and references therein). On the other hand it is well known that there are few, if any, carbon stars with typical AGB luminosities in the Galactic Bulge (quoted in Tyson & Rich 1991), where the metallicity is higher.

3.2. The other constraints

The second constraint is the observed ratio of the number of Galactic carbon-, S- and M-stars on the AGB. This number is taken from Herman (1988) and Jura & Kleinmann (1992a, b). Herman (1988) finds a ratio C/M = 0.18 and S/C = 0.28. Jura & Kleinmann (1992a, b) investigate the number densities and scaleheights of M-, S- and C-rich Miras and semi-regulars (SRs). Although AGB stars are LPVs (long period variables) only during a fraction of their AGB life time (at least in the LMC, see e.g. Paper IV and references therein), the C/M-ratio of LPVs may be indicative for the AGB as a whole. The C-stars, S-stars and the oxygen-rich Miras with periods between 300-400 days and the SR's with periods between 100-150 and 300-400 days all have about the same scaleheight and therefore presumably evolved from the same population. For this data set the ratios of stars are C/M = 0.21 and S/C = 0.30, in good agreement with the earlier estimate.

The third constraint is the observed abundance ratios in Galactic planetary nebulae (PNe). In Paper II we showed that these can constrain the duration of the AGB phase. The abundances are taken from a variety of sources but mainly from Aller & Cryzack (1983), Zuckerman & Aller (1986), Aller & Keyes (1987) and Kaler et al. (1990). The few Halo PNe are not included, since the present calculations concentrate on the galactic disk. The errors in the observed abundances are typically 0.015 in He/H and about 0.2 dex in all other ratios. In the model the abundances of PNe are estimated by averaging the abundances in the ejecta over the final 5 10^4 yr on the AGB. This should be representative of the abundances determined in PNe. The predicted abundances do not change significantly if a lifetime of 2 10^4 yr is adopted. We do not claim that all our model stars will become PNe. Some stars may evolve so slowly in the post-AGB phase that the material ejected during the AGB phase is dispersed before the central star is hot enough to ionize the material. We neglect any changes in the abundances in the post-AGB phase. Although a post-AGB star may experience a late thermal pulse (e.g. Schönberner 1983), possibly changing the abundances, this should be a rare event.

The fourth constraint is the observed initial-final mass relation based on WDs in the solar neighbourhood (for detailed references see Paper I).

The fifth constraint is the birth rate of PNe and the death rate of main sequence stars. Pottasch (1992) quotes a birth rate of PNe of 0.5-2 $\rm yr^{-1}$ in the Galaxy. The fraction of carbon-rich PNe (in the solar neighbourhood) is ~0.6 (Zuckerman & Aller 1986). Assuming that this ratio is a reasonable indicator for the entire Galaxy (one may expect a larger ratio outside the solar circle and a smaller ratio closer to the Galactic centre) we estimate a birth rate of C-rich PNe of 0.3-1.2 $\rm yr^{-1}$.

From the adopted SFR model of van den Hoek et al. (1994) for the Galaxy we derive a (present-day) death rate of carbon stars (initial mass range 1.5-8 $M_\odot$) of 0.36 $\rm yr^{-1}$, calculated from the death rate of main sequence stars. For masses above 1.5 $M_\odot$ (lifetimes $\lesssim$3 Gyr) the SFR is nearly constant (cf. Fig. 1) and the main uncertainty (less than a factor of 2) in the derived birthrate is the absolute value of the observed present-day SFR.

4. Results of the synthetic evolution model calculations

4.1. Basic models

The parameter space in $M_{\rm c}^{\rm min}$, λ and $\eta_{\rm AGB}$ (c.q. $\eta_{\rm BS}$) is investigated. The models that best fit all constraints simultaneously have the following parameters: $M_{\rm c}^{\rm min} = 0.58$ $M_\odot$, $\lambda = 0.75$ (as derived for the LMC in Paper I) and $\eta_{\rm AGB} = 4$, c.q. $\eta_{\rm BS} = 0.08$.

For the Reimers mass loss, there is only a small range in the parameters which can fulfil the constraints. Values for $\eta_{\rm AGB}$ smaller than 4 are not possible since then the initial-final mass constraint is no longer fulfilled (see Fig. 2). Larger values for $\eta_{\rm AGB}$ result in the formation of fewer carbon stars and lower values of the maximum predicted C/O ratio in PNe. In principle, this can be compensated for by decreasing $M_{\rm c}^{\rm min}$ or increasing λ. However, values of $M_{\rm c}^{\rm min}$ below 0.57 $M_\odot$ can be excluded since then nearly all stars go through a carbon star phase, for any reasonable choice of the other parameters. This violates the observed lower limit of ~1.5 $M_\odot$ for carbon star formation. For $M_{\rm c}^{\rm min} = 0.575$ $M_\odot$ and $\lambda = 0.90$, a model with $\eta_{\rm AGB} = 5$ fits the constraints about equally well as the best-fitting model. Models with $\eta_{\rm AGB} \gtrsim 7$ can be excluded since then e.g. the maximum predicted C/O ratio in PNe is only ~3 instead of the observed value of 4 (see Fig. 3) and the ratio of C/M stars is only 0.11 instead of the observed value near 0.2.

The BS mass loss law, allows for a wider range of possible parameters. The value of $\eta_{\rm BS}$ can be as low as 0.03 and still fulfil the observed initial-final mass relation (Fig. 2). A model with $\eta_{\rm BS} = 0.03$, $M_{\rm c}^{\rm min} = 0.59$ $M_\odot$, $\lambda = 0.65$ can fulfil most constraints. However, the average lifetime of the carbon star

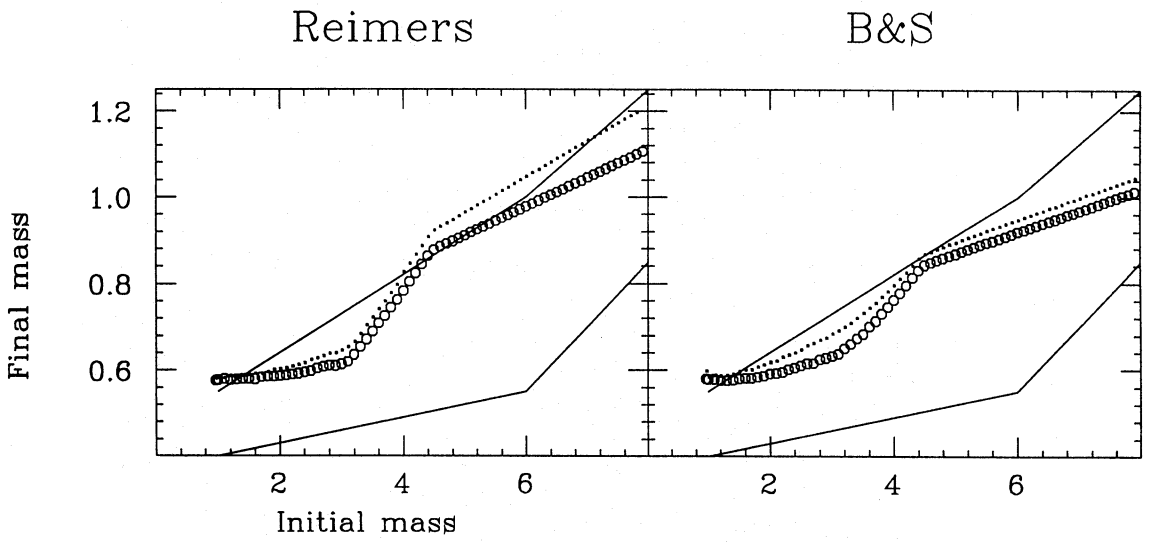

Fig. 2. The initial-final mass relation for Reimers and the BS mass loss. The best-fitting models are represented by the circles, while the minimum and maximum mass allowed for by the observations are indicated by the two lines. For the Reimers law a model with $M_c^{\rm min}$ = 0.58 $M_\odot$, λ = 0.75 and $\eta_{\rm AGB}$ = 2 is also shown (dots); for the BS law a model with $M_c^{\rm min}$ = 0.59 $M_\odot$, λ = 0.65 and $\eta_{\rm BS}$ = 0.03 is also shown (dots)

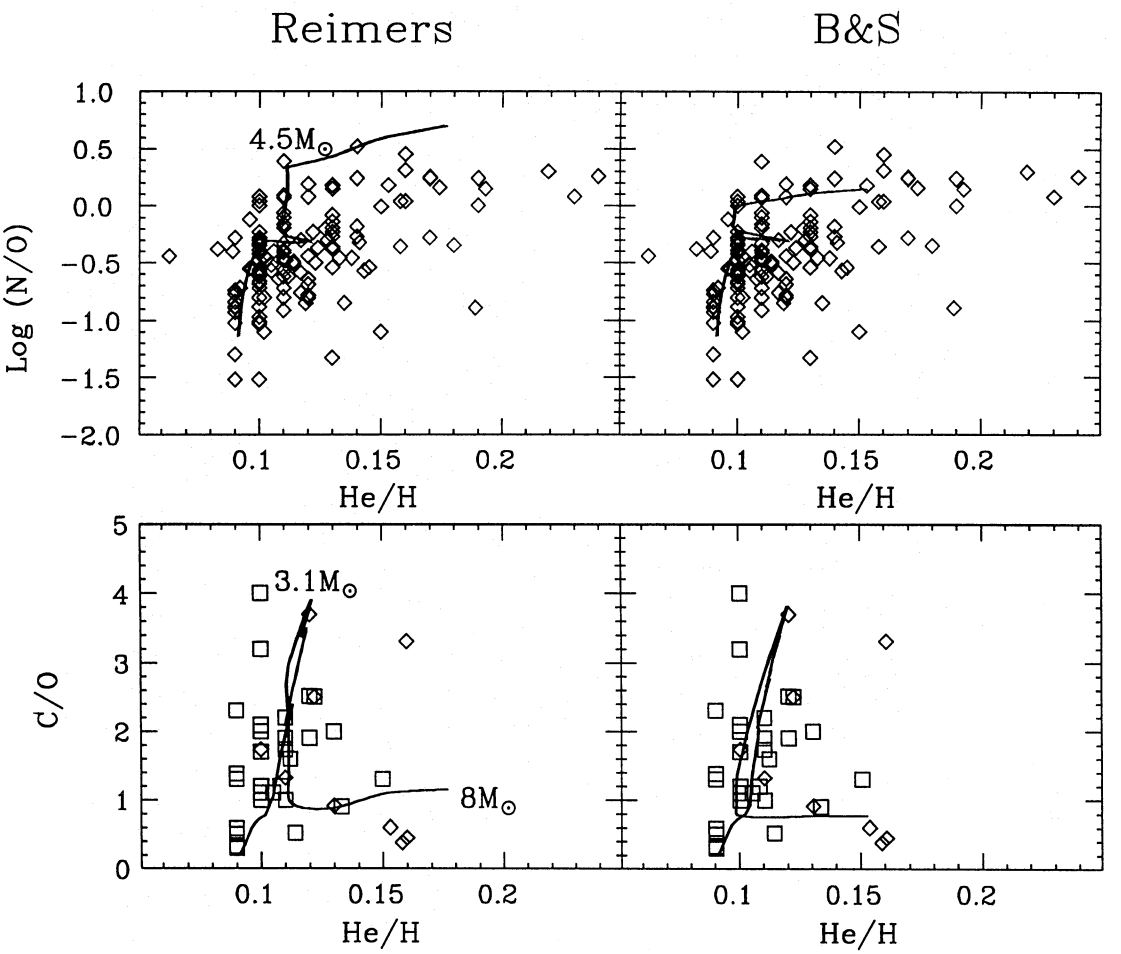

Fig. 3a. The predicted (the solid line) and observed abundance ratios in galactic planetary nebulae (PNe). In the C/O-He/H diagram the observed type I PNe (with N/O>0.5) are indicated by a ◇ and the non-type I PNe by a □. Some initial masses are indicated. For more details see the main text

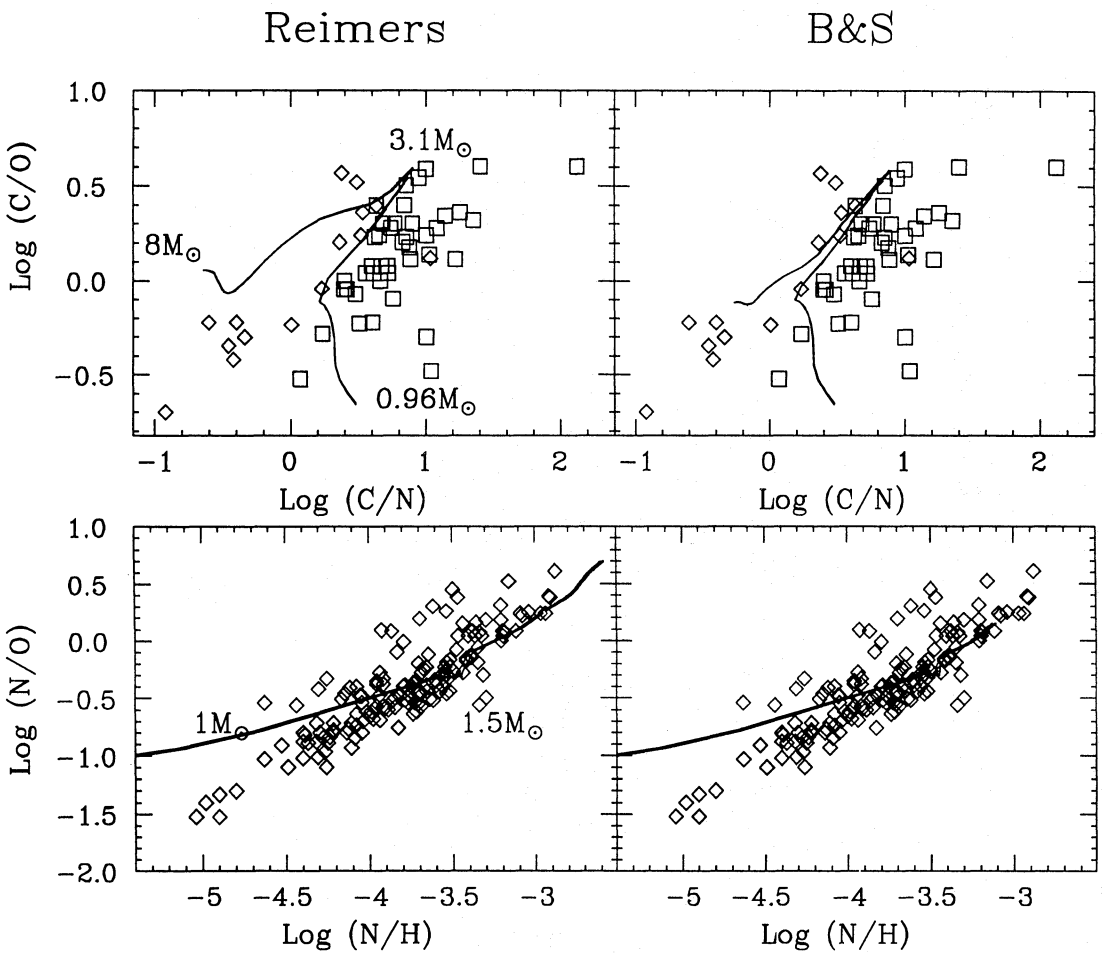

Fig. 3b. (continued) In the C/O-C/N diagram the observed type I PNe (with N/O>0.5) are indicated by a ◇ and the non-type I PNe by a □. In the log (N/O)-log (N/H) panel the 0.96 $M_\odot$ model is outside the plot at –1.13, –6.08. For more details see the main text

phase then becomes so long (35% longer then for the best-fitting model) that the constraint on the birth rate of carbon stars is not fulfilled.

For $M_c^{\min} = 0.573\ M_\odot$ and $\lambda = 0.90$, a model with $\eta_{BS} = 0.16$ can fit all constraints. However, for $\lambda = 0.90$ the increase in the C/O ratio at every thermal pulse is so large that the C/O ratio of $\sim$1.5 $M_\odot$ stars when they turn into carbon stars is larger than 2. However, the largest C/O ratio observed in optical carbon stars is $\sim$1.8 and most have a C/O ratio near 1.2 (Lambert et al. 1986, see the discussion in Sect. 5.3). The best constraint to determine $M_c^{\min}$ and λ is the observed luminosity function of carbon stars (Paper I), which unfortunately is not available in the Galaxy due to the lack of reliable distances. The sensitivity of the M-, S- and C-star LFs to $M_c^{\min}$ and λ is illustrated in Fig. 4.

The best-fitting Reimers and BS model are now discussed in detail. In Fig. 2 the predicted and observed initial-final mass relation are compared for the Reimers and the BS law. Both fit the observations about equally well. Because the BS mass loss law has a stronger luminosity dependence, the mass loss rate for the massive stars is larger than for the Reimers case and vice versa for the low mass stars. That is the reason why the final masses for the massive stars in the BS model are lower than in the Reimers model and vice versa for the low mass stars.

The predicted average mass of the stars when they leave the AGB is 0.578 $M_\odot$ for both the Reimers and the BS mass loss law. This should be compared to the observed mass of the central stars of disk PNe (CSPNe). The mass estimate of CSPNe is hampered by uncertainties in the determination of effective temperature and luminosity but generally most CSPNe have masses between 0.55 and 0.6 $M_\odot$ (Weidemann 1990). The luminosity determination of CSPNe in the Galactic Bulge is less affected by uncertainties in the distance, but the SFR history and metallicity enrichment may be very different from that in the solar neighbourhood. For a sample of CSPNe in the Galactic Bulge Tylenda et al. (1991) quote a mean mass of 0.593 $\pm$ 0.025 $M_\odot$.

A comparison of the predicted final mass of AGB stars with that of White dwarfs (WDs) is not straightforward as WDs, on average, represent an older population so the effects of the star formation history may become important. However, this effect appears not to be large. From Bergeron et al. (1992) we calculate for 112 WDs with masses between 0.45 and 1 $M_\odot$ (the WDs with lower masses are thought to have originated from binary evolution) that the average mass is 0.583 $M_\odot$.

Table 2. Results for individual stars

M ($M_\odot$)	Z	P (%)	model	TM	TS	TC (10^3 yrs)	TAGB	N_c	N_{tot}	$\dot{M}_{AGB}$ (10^{-6} $M_\odot$/yr)	C/O [1]	$^{12}C/^{13}C$ [1]	C/O [2]	$^{12}C/^{13}C$ [2]
0.97	0.0008	0	Re	486	0	0	486	-	3	0.43	-	-	0.23	23
			BS	544	0	0	544	-	3	0.43	-	-	0.23	23
1.0	0.0033	29.2	Re	206	0	0	206	-	3	0.91	-	-	0.35	23
			BS	232	0	0	232	-	3	0.80	-	-	0.35	23
1.2	0.0107	74.2	Re	281	0	0	281	-	4	1.38	-	-	0.67	23
			BS	264	0	0	264	-	4	1.47	-	-	0.67	23
1.4	0.0171	85.5	Re	358	0	0	358	-	5	1.70	-	-	0.78	23
			BS	324	0	0	324	-	5	1.88	-	-	0.78	23
1.45	0.0178	87.0	Re	359	0	28	386	6	6	1.73	5.02	219	5.02	219
			BS	338	0	0	338	-	5	1.97	-	-	0.79	23
1.5	0.0181	88.2	Re	356	0	52	407	6	6	1.77	2.38	80	2.38	80
			BS	351	0	0	351	-	5	2.06	-	-	0.80	23
1.55	0.0182	89.2	BS	355	0	37	392	6	6	1.99	1.59	50	1.59	50
1.6	0.0182	90.1	Re	354	0	106	460	6	7	1.82	1.47	45	7.47	433
			BS	354	0	62	416	6	6	2.01	1.27	39	1.27	39
1.75	0.0183	92.5	Re	354	0	204	558	6	8	1.80	1.16	35	7.81	480
			BS	354	0	173	527	6	7	1.90	1.07	32	1.47	46
2.0	0.0185	95.3	Re	352	91	310	753	7	10	1.71	1.28	40	6.50	341
			BS	352	91	367	810	7	10	1.59	1.18	36	2.08	70
2.5	0.0188	97.5	Re	351	91	773	1214	7	15	1.52	1.03	33	4.08	171
			BS	351	91	1166	1607	7	20	1.15	1.00	32	3.26	126
3.0	0.0189	98.6	Re	437	185	1001	1623	9	21	1.43	1.08	36	4.33	194
			BS	437	185	1667	2289	9	31	1.00	1.04	35	3.54	147
3.5	0.0191	99.2	Re	106	119	746	971	8	28	2.80	1.05	34	6.12	332
			BS	106	119	640	865	8	25	3.15	1.04	34	3.00	119
4.0	0.0191	99.6	Re	55	83	537	675	11	48	4.56	1.01	33	3.69	155
			BS	55	83	183	321	11	22	9.66	1.01	33	1.57	55
5.0	0.0191	99.9	Re	391	161	0	552	-	129	6.97	-	-	0.86	16
			BS	140	0	0	140	-	29	27.9	-	-	0.75	20
7.0	0.0192	99.9	Re	181	281	113	575	326	444	9.32	1.00	15	1.13	13
			BS	99	0	0	140	-	55	54.9	-	-	0.77	20

Notes. (1) the C/O ratio and the $^{12}C/^{13}C$ ratio at the thermal pulse when the star becomes a carbon star, (2) the C/O ratio and the $^{12}C/^{13}C$ ratio at the end of the AGB.

Listed are the initial mass, the initial metallicity, the cumulative probability to find a star on the AGB with a mass between M_{lower} and M, the type of model (Re = Reimers, BS = Blöcker & Schönberner), the lifetime of the M, S, C and the total AGB phase, the pulse number at which the star becomes a carbon star, the total number of thermal pulses on the AGB and the average mass loss rate on the AGB.

In Fig. 3 the observed and predicted abundances in PNe for the two best models are compared. We expect to find three distinct groups of stars. The first group consists of stars with initial masses less than about M_1. The stars with $M < M_1$ do not experience the second dredge-up and have core masses too low for the third dredge-up to occur. In these stars we expect to see the main sequence abundances changed by the first dredge-up process only. The mass M_1 must be somewhat lower than the lower mass limit of carbon star formation and is found to be $M_1 \approx 1.5$ $M_\odot$. The second group consists of stars in the initial mass range $M_1 \lesssim M \lesssim M_2$. After the first dredge-up (and maybe second dredge-up for the massive ones) these stars dredge-up carbon, helium and some oxygen on the AGB during thermal pulses (third dredge-up). We expect the C/O and He/H ratios to be enhanced. The third group consists of stars initially more massive than about M_2. In these stars, the carbon dredged-up during thermal pulses is largely converted to nitrogen by hot-bottom burning (HBB; see Paper I) and no carbon stars are formed. In the present calculations we find that M_2 is about 4 $M_\odot$.

In the N/O-He/H panel the main difference between the Reimers and the BS model is in the predicted N/O ratio for masses above 4.5 $M_\odot$. Both models fail to predict He/H ratios larger than 0.2. This may be due to the adopted parameterization of HBB. Alternatively the mass loss rate for the highest intial masses is overestimated. In the C/O-He/H panel the main difference is in the C/O ratio of the most massive stars. The Reimers model predicts C/O $\gtrsim$1 while the few observations (the $\diamond$'s near He/H = 0.16) seem to favor the BS model. In the C/O-C/N panel the differences are small. Both models predict too small C/N ra-

tios for a given C/O ratio in the mass range 1.5-3 $M_\odot$. In the N/O-N/H panel differences are small. Most interestingly, for M $\lesssim$1.5 $M_\odot$ the relation between N/O and N/H is determined by the age-metallicity relation of N and O for main sequence stars. Stars in this mass range do not experience a third dredge-up and the effects of the first dredge-up are not very mass dependent. The predicted position of the 0.96 $M_\odot$ model is off the plot at log (N/O) = –1.13, log (N/H) = –6.08. The lowest observed log (N/H) ratio is –5.0. There are several explanations for this discrepancy: (1) The adopted age-metallicity relation for N and/or O for M $\lesssim$1 $M_\odot$ ($\gtrsim$10 Gyr) is incorrect, (2) stars below $\lesssim$0.98 $M_\odot$ do not reach the AGB either because mass loss prior to the AGB has ended their life prematurely (this would imply that $\eta_{\rm RGB}$ is higher than assumed) or because the age of the Galaxy (c.q. the Galactic disk) is less than 14 Gyr ($M_{\rm lower} \approx 0.98$ $M_\odot$, corresponding to an age of about 13 Gyr, instead of 0.96 $M_\odot$). Alternatively, (3) stars do reach the AGB but do not form a PN (the nebulae are dispersed before the central star is hot enough to ionize them; Schönberner 1983), or (4) have so far not been observed (due to their expected low surface brightnesses). A combination of the last two arguments seems the most plausible.

The predicted ratio of stars for both mass loss models is C/M = 0.15 and S/C = 0.13. Both ratios are somewhat below the observed values. The C/M ratio is sensitive to the SFR during the first 10 Gyr and the AGB lifetime of the stars with the lowest initial masses that reach the AGB. The S/C ratio is sensitive to the adopted C/O ratio where the M to S transition occurs.

In Table 2 the results for individual masses are listed for the two best models. A discussion on the C/O and $^{12}C/^{13}C$ ratio is postponed to Sect. 5.3. With the BS law carbon stars are predicted above 1.55 $M_\odot$, for the Reimers law this is 1.45 $M_\odot$. This is in good agreement with observations. The model predicts that stars in the range 1.5 $M_\odot \lesssim M \lesssim 1.6$ $M_\odot$ become carbon stars at their last thermal pulse (TP) on the AGB and live only a few 10^4 yr as carbon stars. More massive stars experience additional TPs as carbon stars and live up to 10^6 yr. For both mass loss models S-stars originate from slightly more massive stars (M $\gtrsim$2 $M_\odot$). A similar results was found for the LMC (Paper I) in agreement with observations of S-stars in LMC clusters. For the Galaxy one might argue (Sect. 2) that S- and C-stars originate from roughly the same population. If future observations would confirm this, this could mean that λ increases with core- and/or initial mass. For smaller λ the increase in the C/O ratio at every thermal pulse is less, increasing the probability that the star will go through an S-star phase.

The mean carbon star lifetime, averaged over the probability to find a star of a given mass in the carbon star phase, is 3.0 10^5 yr for the Reimers mass loss law and 4.4 10^5 yr for the BS law. The carbon star lifetime we derive is much longer than estimated in Groenewegen et al. (1992). This is due the assumption in Groenewegen et al. (1992) that the thermal pulse that forms the carbon star is also the last thermal pulse for all AGBs. We show here that carbon stars can experience additional thermal pulses.

The observed surface density in the galactic plane of carbon stars in the solar neighbourhood depends on the assumed mean luminosity. For a value of 7050 $L_\odot$ the local surface density is 85 kpc^{-2} (Groenewegen et al. 1992). The main contribution to the surface density comes from optical carbon stars with a 60 μm excess (Groenewegen et al. 1992). As the lifetime of the detached shell causing the 60 μm excess is $\lesssim$2 10^4 yr, these stars could well have a luminosity below the mean, since they still could be in the luminosity dip of the thermal pulse cycle. If the luminosity of the optical carbon stars with a 60 μm excess were 5000 $L_\odot$ then the total surface density of carbon stars would be 130 kpc^{-2} (Groenewegen et al. 1992). Thronson et al. (1987) and Jura et al. (1989) found no gradient of carbon stars along the galactocentric axis on a scale of at least 4 kpc. If the surface density of carbon stars is constant throughout the Galaxy we estimate a total number of 9 10^4 carbon stars in the Galaxy (if σ = 130 kpc^{-2}). Using the mean lifetime derived above, we estimate a birth rate of carbon stars of 0.31 and 0.21 carbon stars yr^{-1} in the Galaxy for the Reimers and the BS law, respectively. Both values agree with the observed rate (0.3-1.2 yr^{-1}) considering the uncertainty in both the predictions and observations (see Sect. 3.2).

4.2. Sensitivity of the results to the adopted SFR and AMR

In the calculations in the previous subsection we adopted a specific SFR and AMR, taken from a preliminary model of van den Hoek et al. (1994). The iron abundance of this specific model is in good agreement with the few observational data on carbon stars. Lambert et al. (1986) derived a range of –0.3 $\lesssim$[Fe/H] $\lesssim$0. For a typical carbon star initial mass of 2 $M_\odot$ we find that the model has [Fe/H] = –0.05. In addition, the present-day oxygen abundance of the adopted AMR is 8.76 (on a scale with H = 12), in good agreement with observations (see the discussion in Peimbert et al. 1993).

When this work was essentially completed the latest models of van den Hoek (1994) became available, including SFR models with an initial burst and thereafter an exponential decline, and including gas infall which were found to be in best overall agreement with the observations (for details see further van den Hoek et al.). Also the effect of metallicity on the main-sequence lifetimes is consistently taken into account in these new models. This effect lowers the initial mass of stars that can reach the AGB in 14 Gyr to about 0.82 $M_\odot$compared to 0.97 $M_\odot$ adopted in this paper. The overall metallicity in these new models is higher than in the model adopted in Sect. 4. In particular, for a 2 $M_\odot$ star [Fe/H] is about 0.12 and the present-day oxygen abundance is 9.03 (the models of van den Hoek et al. were not tuned to fit the abundance data on AGB stars, but fit many other constraints). Although the adopted AMR appears to be in better agreement with the (sparse) observations of carbon stars it may be useful to give the effects on the results if the new SFR and AMR models are used.

The changes are two-fold and related to the overall higher metallicity and combined effect of a change in the SFR and $M_{\rm lower}$, respectively. For a Reimers mass loss law and the best parameter set of $M^{\rm min}$ = 0.58 $M_\odot$, λ =0.75 and $\eta_{\rm AGB}$ = 4 the AMR relation with a higher metallicity results in the formation

of fewer carbon stars, c.q. stars become carbon stars in a later phase of AGB evolution: the lower limit of carbon star formation is raised to 1.7 $M_\odot$ and the maximum predicted C/O ratio is PNe is only about 2.5. We tried to find a set of parameters to bring the predictions in accordance with the observations. A model with $M^{\rm min}$ = 0.585 $M_\odot$, λ = 0.75 and $\eta_{\rm AGB}$ = 2.5 fits the observed lower mass limit of carbon star formation of 1.5 $M_\odot$ and the observed maximum C/O ratio in disk PNe of about 4. However, the lower mass loss rate implies much longer (average) lifetimes (by 50% compared to the best model of the previous section) resulting in a death rate of carbon stars which is below the observed value. In addition, the longer lifetimes imply more thermal pulses and more dredge-up of helium. This affects in a negative way the comparison with the observation in the C/O-He/H and N/O-He/H diagrams. In conclusion, models with a higher metallicity fit the observations less well than the AMR adopted in Sect. 4.1

The overall probability to be on the AGB as a star with an initial mass larger than 1.5 $M_\odot$, which depends on the IMF the SFR and the intrinsic AGB lifetimes, is higher than in the model used in Sect. 4.1 and therefor the C/M ratio is higher. In fact, whereas for the final parameter set derived in Sect. 4.1 the C/M ratios were on the low side of the observed range, for the new sets the C/M ratios are typically in the range 0.4-0.9, larger than observed. This underlines the sensitivity of the C/M ratio to the SFR, IMF and AGB lifetimes.

The discrepancy in the N/O-N/H diagram (cf. Fig. 3) between the predicted and observed abundances of PNe for log (N/H) $\lesssim$–5 remains with the new AMRs. If metallicity dependent lifetimes are used, PNe with log (N/H) = –5 are predicted from a star with an initial mass of about 0.84 $M_\odot$. This corresponds to an age of 13 Gyr, identical to the result found before.

The predicted LFs are sensitive to both the AMR and the SFR (for a fixed set of parameters $M^{\rm min}$, λ and $\eta_{\rm AGB}$). Since the probability to be a massive AGB star is larger than for the model used in Sect. 4.1 the LFs are shifted to higher luminosities. The peak of the C-star LF occurs at $M_{\rm bol}$ = –5.1 (instead of $M_{\rm bol}$ = –4.9; see discussion below in Sect. 5.2). The peak of the M-star LF occurs at $M_{\rm bol}$ = –4.6 (instead of $M_{\rm bol}$ = –4.1). The main change in the M-star LF is in the high-luminosity tail. For the models in Sect 4.1 only a small percentage (about 0.5%) of M-stars was predicted to occur at $M_{\rm bol} < -5.4$. For the new SFR and AMR models this is about 4%. In Sect. 5.2 we estimate that for oxygen-rich Miras the observed fraction with $M_{\rm bol} < -5.4$ is about 0.1% to which a small percentage of OH/IR stars should be added. The high C/M ratio and the large fraction of M-stars at high luminosity argue against the new SFR, which predicts relatively more massive stars.

5. Discussion

5.1. The initial mass range of carbon stars

We conclude that only stars in the initial mass range ~1.5 to ~4 $M_\odot$ will become, for some time, carbon stars. Some of the Reimers models above 4 $M_\odot$ also end as carbon stars. The lower limit is derived strictly from observational evidence (Sect. 3.1). The observational evidence for the upper limit is less constraining. In the model the upper limit of about 4 $M_\odot$ occurs naturally when hot-bottom burning becomes active. The upper limit is sensitive to the amount of hot-bottom burning.

In two recent papers, the mass range of carbon stars was addressed in a different context. Barnbaum et al. (1991a) concentrated on the population of carbon stars with expansion velocities $\geq$17.5 km s^{-1}. She found (see also earlier work quoted by her) that these objects are concentrated toward the galactic plane ($|\ b\ | < 20°$) and derived a scaleheight of 107 pc, corresponding to an initial mass range of 2.5-4 $M_\odot$. She derived typical luminosities of 1.5 10^4 $L_\odot$.

Kastner et al. (1993) observed CO emission from a sample of distant (predominantly) AGB stars at low Galactic latitude ($|\ b\ | \lesssim 3°$). The longitude of the sample stars was chosen such that more or less reliable kinematical distances could be derived. They found similar luminosities for carbon stars and oxygen-rich stars of 1.3-2 10^4 $L_\odot$ (–5.6 $\lesssim M_{\rm bol} \lesssim$–6.0) and concluded that the initial mass of the carbon stars in their sample was at least 2 $M_\odot$. The average expansion velocity of the carbon stars in their sample was 17.5 $\pm$ 1.0 km s^{-1}, consistent with that found by Barnbaum et al.

Although our model does not predict kinematical (distances from the Galactic plane) or circumstellar properties (expansion velocities) for carbon stars, there appears to be at least qualitative agreement between our work and that of Barnbaum et al. and Kastner et al. We predict a population of carbon stars in the range 2-4 $M_\odot$ which is more massive than the average carbon star (about 1.8 $M_\odot$). These dominate the high-luminosity tail of the luminosity function and have luminosities up to $M_{\rm bol}$ = −6.4 (see additional discussion below). It is only natural that these 'massive' carbon stars are preferentially found at low z. From recent calculations (Habing et al. 1994) it is predicted that, at least to some extent, the outflow velocity increases with increasing luminosity in a flow driven by radiation pressure on dust.

The referee pointed to the object OH 231.8+4.2, which is considered to be an oxygen-rich star on the verge of becoming, or already being, a proto-planetary nebula (PPN). This object apparently belongs to the open cluster M46 which has a turn-off mass of 3 $M_\odot$ (Jura & Morris 1985). Since the lifetime from the turn-off point to the end of the AGB phase is non-negligible we estimate from different evolutionary calculations (Boothroyd & Sackmann 1988; Castellani et al. 1990; Lattanzio 1991) that the initial mass of OH 231.8, if it is a member of M46, may be as high as 3.7 $M_\odot$. This mass is close to our predicted upper limit. In addition, OH 231.8+4.2 could experience another thermal pulse in the future, possibly changing it into a carbon star. Finally we note that OH 231.8+4.2 may be a close binary system which may have resulted in a peculiar evolution. At present we do no see a serious conflict with our prediction for the upper limit of carbon star formation. Nevertheless, it may be useful to stress that we predict all stars between ~1.5 and ~4 $M_\odot$ to end the AGB as carbon-stars. Any definite oxygen-rich PPN with a mass clearly below 4 $M_\odot$ (and above 1.5 $M_\odot$) would be in conflict

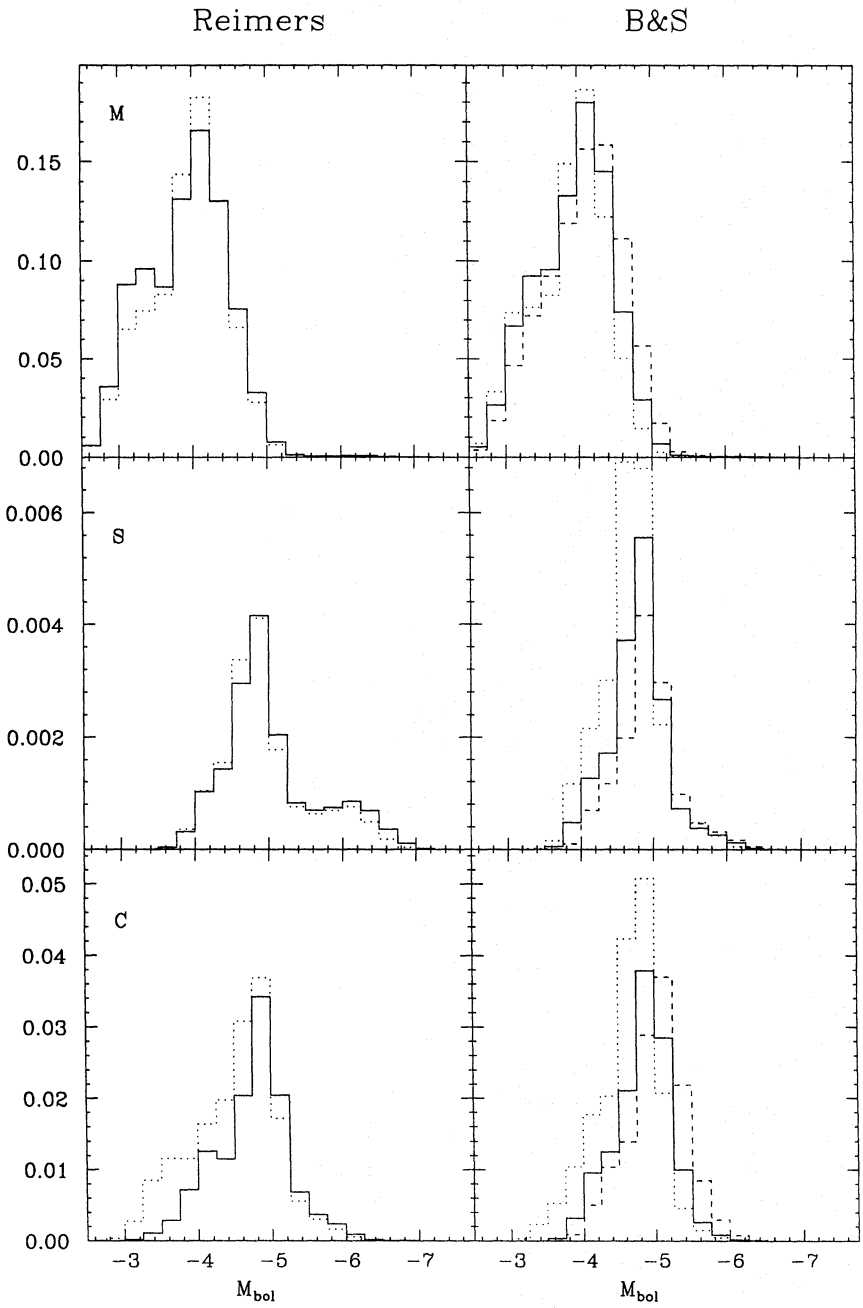

Fig. 4. The predicted luminosity functions of M-, S- and C-stars for the best-fitting BS and Reimers mass loss models (solid lines). For the Reimers law a model with $M_c^{\rm min} = 0.575\ M_\odot$, $\lambda = 0.90$ and $\eta_{\rm AGB} = 5$ is also shown (dotted line); for the BS law, models with $M_c^{\rm min} = 0.573\ M_\odot$, $\lambda = 0.90$ and $\eta_{\rm BS} = 0.16$ (dotted line) and $M_c^{\rm min} = 0.59\ M_\odot$, $\lambda = 0.65$ and $\eta_{\rm BS} = 0.03$ (dashed line) are also shown. The sum over all bins is unity

with the predictions of the model. In such a case, one may have to consider more complicated models and for example abandon the simplifying assumption of a constant dredge-up efficiency.

5.2. The predicted luminosity function of AGB stars

In Fig. 4 the predicted luminosity functions (LFs) of M-, S- and C-stars are given for the two best-fitting models (solid lines) and some additional models (dotted and dashed lines). There are no major differences between using the BS and the Reimers mass loss law. The peak of the carbon star LF occurs at the same luminosity as in the LMC (see Paper I), providing support for the assumption in Groenewegen et al. (1992) and Groenewegen (1994a) of a mean luminosity of 7050 $L_\odot$ for Galactic carbon stars. The peak of the oxygen-rich TP-AGB stars occurs at 3450 $L_\odot$. This is in reasonable agreement with the value of 4000 $L_\odot$ determined by Habing (1988) by modelling the space distribution of AGB stars. The luminosity of a typical Galactic AGB star is in any case less than the 10^4 $L_\odot$ often assumed (e.g. Jura & Kleinmann 1989).

An alternative way to study the luminosity function of carbon- and M-stars is through the period distribution of Miras and employing a period-luminosity (P-L) relation to convert the period distribution into a luminosity function. The second step is then to construct a volume-complete sample as Miras with large periods are more luminous and sample a larger volume.

For the carbon Miras we have performed these steps (Groenewegen 1994b) and find a mean luminosity of 8200 ± 1500 $L_\odot$, in good agreement with the theoretical prediction of 7050 $L_\odot$.

For oxygen-rich Miras we proceeded in a similar way as for the carbon Miras. From the General Catalog of Variable Stars (Kholopov et al. 1985) all Miras were selected. Not considered were Miras with spectral types C or S, stars with an uncertain Mira classification and stars with no or uncertain periods. The sample does include a fair number of Miras of unknown spectra type. For these we checked if they had silicon carbide emission in their LRS spectra, if available. One source was eliminated in this way. The final sample consists of 3991 Miras. The periods range from below 50 days (2 stars) to 860 days. This indicates that many OH/IR stars with periods in excess of 1000 days are not represented here. On the other hand their space density is expected to be small and probably does not influence the analysis. The periods were binned in 50 days intervals. The median period is 274 days. However, Miras with larger period are more luminous on average than Miras with smaller periods. This effect tends to decrease the median period of a volume complete sample compared to the straight median calculated above. To correct for the difference in limiting volumes the period-luminosity relation of Feast et al. (1989) for oxygen-rich Miras in the LMC was used. This relation was derived for periods below 420 days, but will be assumed to hold for larger periods as well. Only 6.5% of all Miras in the sample have periods above 420 days, so the uncertainty in the P-L relation for this period range is unlikely to affect the results discussed below.

To convert the P-L relation to the Galaxy a distance modules of 18.5 ± 0.1 is assumed, and, following Whitelock (1994), no correction for the difference in metallicity is made. The final relation reads: $M_{\rm bol}$ = –3.00 log P + 2.85. As can be easily shown the relative correction factors only depend on the slope d$M_{\rm bol}$/dlog P and not on the zeropoint of the P-L relation. The relative, volume-corrected period distribution was calculated by dividing the number of stars in each bin by $L^{1.5}$, where the luminosity was calculated from the P-L relation for the center period of each bin. The median period of the volume corrected period distribution is 224 days. The exponent of 1.5 in the correction factor assumes that the limiting volume depends on (distance)^3. This is valid if the limiting distance is smaller than the typical scaleheight. If the limiting distance is larger than the scale height the limiting volume scales like (distance)^2. In that case the median period of the volume corrected sample will be inbetween 224 and 274 days. Adopting 235 ± 10 days as the mean period and taking into account an error of 0.1 in the zeropoint of the P-L relation a mean luminosity of oxygen-rich Miras of 3900 ± 450 $L_\odot$ is derived, in good agreement with the theoretical estimate.

A similar analysis was performed by Wood & Cahn (1977). However, they first of all included Miras of all spectral types (whereas it is demonstrated here that carbon Miras are more luminous on average than oxygen-rich Miras) and second of all only included Miras with distances to the Galactic plane of less than 200 pc, which should have biased their sample to more massive Miras. The peak of their period distribution (based on 511 stars) occurred at about 350 days.

The referee noted that the high-luminosity cut-off of M-stars in Fig. 4 appears to occur at $M_{\rm bol} \approx -5.4$ and questioned the reality of it. In fact, M-stars are predicted to exist upto $M_{\rm bol} = -7.1$, the traditional limit of AGB luminosity. The percentage of M-stars with $M_{\rm bol} < -5.4$ is predicted to be about 0.5%. From the volume-corrected period distribution discussed above we derive that the percentage of oxygen-rich Miras with $M_{\rm bol} < -5.4$ (corresponding roughly to periods above 550 days) is 0.1%. To this should be added an unknown, but expected to be small, percentage of OH/IR stars; there does not appear to be a conflict between observations and our predictions regarding the existence of high-luminosity M-stars.

The M- and S-star LFs are relatively insensitive to changes in the dredge-up parameters $M_{\rm c}^{\rm min}$ and λ. As shown in Paper I, the carbon star LF is sensitive to those parameters, in the sense that $M_{\rm c}^{\rm min}$ mainly influences the low-luminosity tail of the LF, and λ mainly the location of the peak of the LF. When distances to AGB stars become available as a result of the Hipparcos mission, the predicted LFs can be tested. If the observed luminosity function of a volume complete sample of carbon stars is available then the values of $M_{\rm c}^{\rm min}$ and λ can be determined more accurately than is possible at present.

5.3. The evolution of the C/O ratio in AGB stars

Since PNe evolve from AGB stars, it is interesting to compare the ratio of their C and O abundances. For the Galaxy they have been compared by Smith & Lambert (1990). They note that while the C/O ratio in (disk-) PNe ranges up to about 4 (cf. Fig. 3), the maximum observed C/O ratio in carbon stars is only about 1.5 (Lambert et al. 1986). Smith & Lambert suggest that systematic errors, the obscuration of more carbon-rich stars by dust and the possibility that C-rich PNe receive their enrichment just before the superwind strips the AGB star of its envelope, as possible explanations.

Dust obscuration seems not very likely. In Paper I we showed, based on the observed number of IRAS sources in the LMC, that dust obscuration cannot be very important in the LMC. For the Galaxy, Groenewegen & de Jong (1993b) showed that in a sample of fourteen infrared carbon stars, eight in fact have optical counterparts.

In Fig. 5 we show the evolution of the C/O ratio on the AGB for the best-fitting Reimers and BS models for stars of 1.5 $M_\odot$ (Reimers law, upper left panel), 1.55 $M_\odot$ (BS law, upper right panel), 2 $M_\odot$ (Reimers law, middle left; BS law, middle right panel) and 4 $M_\odot$ (Reimers law, lower left; BS law, lower right panel). The 1.5 and 1.55 $M_\odot$ star skip the S-star phase and become carbon stars at their last thermal pulse on the AGB. The C/O ratio after the star turns into a carbon stars is 2.4 for the Reimers 1.5 $M_\odot$ model and 1.6 for the BS 1.55 $M_\odot$ model. A C/O ratio of 2.4 is in disagreement with observations. The largest C/O ratio in the Lambert et al. sample is 1.76. The BS 1.55 $M_\odot$ model represents the upper range of the observed parameter space. If λ would be smaller than 0.75 at small core

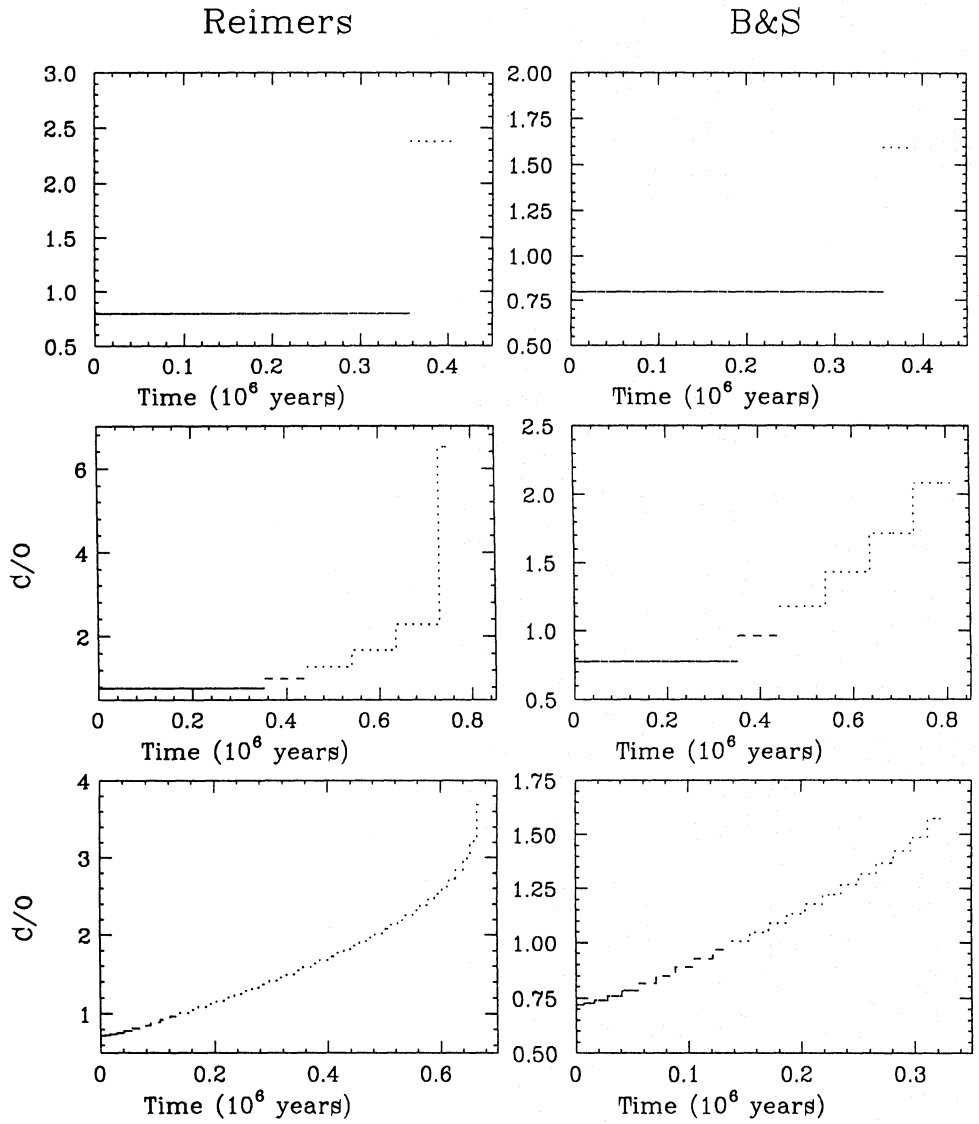

Fig. 5. The predicted evolution of the C/O ratio for the best-fitting BS and Reimers mass loss models. Indicated are the evolution of a 1.5 (upper left), 1.55 (upper right), 2 $M_\odot$ (middle panels) and 4 $M_\odot$ models (lower panels). The M-, S- and C-star phase are represented by the solid, dashed and dotted line respectively

masses (see the argument in the previous section) then the C/O ratio would be smaller when the star becomes a carbon star.

The 2 $M_\odot$ model stars evolve through the S-star phase before becoming carbon stars. They experience three additional thermal pulses increasing their C/O ratio. With the Reimers law it experiences a late thermal pulse at low envelope mass which increases the C/O ratio significantly. This shows that the suggestion by Smith & Lambert that C-rich PNe receive their enrichment at the very end of the AGB can play a role in some cases. The 4 $M_\odot$ models behave in a similar way as the 2 $M_\odot$ models except that the interpulse period is shorter and therefore the stars experience a larger number of thermal pulses.

A comparison of the observed range in the C/O (1.0–1.76) and $^{12}C/^{13}C$ ratio (20-100; excluding the J-type stars) in the Lambert et al. sample with the predicted C/O and $^{12}C/^{13}C$ ratios in Table 2 suggest that only carbon stars during their first few pulses (depending on initial mass) are represented in the Lambert et al. sample.

Willems & de Jong (1988) and Groenewegen et al. (1992) have classified carbon stars in groups II to V. Group II C-stars have a 60 μm excess indicating a phase of high mass loss in the past, group III stars have a moderate present-day mass loss and groups IV and V are infrared carbon stars with a high present-day mass loss rate. Group I consists of carbon stars with a peculiar evolutionary history (e.g. Barnbaum et al. 1991b). Groenewegen et al. (1992) assumed that most Galactic carbon stars have a similar initial mass, loop only once in the IRAS color-color diagram, and that groups II-V represent an evolutionary sequence. This working hypothesis needs refinement.

Of the 30 stars with a C/O ratio determined by Lambert et al., 90% belong to group II and the remaining 10% to group III. Yet, disk PNe are known with C/O ratios up to about 4. This implies first that carbon stars with C/O $\gtrsim$1.5 are to be found among groups III, IV and V, and secondly that stars with C/O $\gtrsim$1.5 do not make loops through the IRAS color-color diagram. Only for one infrared carbon star has a C/O ratio been estimated. For IRC 10216 (a group IV star) a ratio C/O $\approx$ 2.5 has been inferred

based on its molecular emission lines (Morris 1975; Mitchell & Robinson 1980). The carbon stars with C/O ratios $\gtrsim$1.5 are predicted to show $^{12}C/^{13}C$ ratios in excess of 30-80 as observed in the Lambert et al. sample for C-stars with C/O less than $\sim$1.5.

From our model we find that there is a 29% probability for carbon stars to have a C/O ratio of $\gtrsim$1.5 (based on Table 2). The observed ratio of the surface density of groups III, IV and V to all carbon stars is 14-21%, depending on the assumed luminosity (Groenewegen et al. 1992). This is roughly consistent with the proposition that groups III, IV and V represent the population of carbon stars with C/O $\gtrsim$1.5. On average, carbon stars with C/O $\gtrsim$1.5 (group III, IV and V stars) represent a more massive population than carbon stars with C/O $\lesssim$1.5 (group II stars). The scale height of the different groups (Groenewegen et al. 1992) and the fact that at least some infrared carbon stars have luminosities above the mean (based on their pulsation period; Groenewegen 1994a, b) substantiate this.

Stars with C/O $\gtrsim$1.5 apparently do not become optical carbon stars with a 60 μm excess. Based on theoretical radiative transfer models (e.g. Chan & Kwok 1988) this requires that the mass loss rates during and after the thermal pulse do not differ by a large factor (for group II stars the mass loss rate during and after a thermal pulse are on the order of 10^{-5} and 10^{-7} $M_\odot$/yr, respectively) and that the time for a phase of new significant mass loss to start is rather short (for group II stars this is about 1-2 10^4 years). Since both the duration of the thermal pulse (identified with the phase of high mass loss), the increase in surface luminosity during the thermal pulse, and the duration of the subsequent luminosity dip (identified with the phase of low mass loss) decrease with increasing core mass (i.e. initial mass) it may be possible that massive stars do not show significant loops after a thermal pulse and would therefore not reach the location of the group II stars.

5.4. Are the detached shells around carbon stars carbon-rich ?

The possibility that the chemical composition of the circumstellar shells of some carbon stars could be *oxygen-rich* was originally stirred by the discovery of silicate features in the LRS spectra of a few carbon stars (Willems & de Jong 1986; Little-Marenin 1986). Later on, Willems & de Jong (1988) proposed a scenario for carbon star evolution related to the occurrence of thermal pulses. In this scenario, the oxygen-to-carbon transition causes the mass loss to drop and the oxygen-rich circumstellar shell to expand and dilute. This gives rise to the characteristic excess at 60 μm observed in many optical carbon stars. Although it now appears that the unusual evolutionary history of carbon stars with silicate features is unrelated to the carbon stars with 60 μm excess, and may possibly be explained by an oxygen-rich circumstellar disk around a carbon star (see Engels & Leinert 1994 and references therein) the chemical composition of the shells around the carbon stars with 60 μm excess remains an interesting question. We have suggested that sub-mm observations may resolve the question whether the shells are carbon-rich or oxygen-rich (Groenewegen & de Jong 1994a).

In a recent paper, Zuckerman (1993) has claimed that the detection of HCN around some carbon stars with 60 μm excess indicates that the detached shells are carbon-rich. This argument is flawed. From the calculations of Olofsson et al. (1990), and of Bergman et al. (1993) for S Sct, it follows that HCN is destroyed at radii corresponding to expansion time scales of $\lesssim 10^3$ yr. The inner radii of the dust shells which cause the 60 μm excesses are located at distances corresponding to timescales of $\sim 10^4$ yr (Olofsson et al. 1993). The presence of HCN in these stars is most likely due to present-day carbon-rich mass loss and not related to the detached shell.

Zuckerman continues to point out that the Willems & de Jong (1988) scenario predicts that when the 12 and 25 μm fluxes are entirely photospheric, the 60/25 ratio decreases as the dust shell moves further out. This is true. However, this is also the case if the detached dust shell were carbon-rich, as is Zuckerman's preferred model. The fact that the double-peaked CO line profiles are found in a few stars with moderate 60/25 ratios, but not in carbon stars with lower 60/25 ratios, therefore is not an indication of the incorrectness of the Willems & de Jong model, as claimed by Zuckerman, but due to a mechanism which prevents the occurrence of double-peaked CO profiles in stars with moderate 60/25 ratios, independent of the chemical composition of the detached shell.

This mechanism is most probably photodissociation. The calculations of Bergman et al. (1993) for S Sct show that the detached CO shell will survive for only another few thousand years. As the evolution towards lower 60/25 ratios is very slow, it is not clear that stars with a small 60 μm excess should still show a double-peaked CO line profile. The time scale a detached CO shell can avoid photodissociation depends on the product of the mass loss rate in, and the duration of, the phase of high mass loss rate, and on the interstellar radiation field. For S Sct, an UV field twice the standard value reduces the lifetime of the CO shell from $\sim$1.2 10^4 to $<10^4$ yr (Bergman et al. 1993). As the mass loss rate that caused the detached shell in S Sct is probably higher than in other carbon stars with 60 μm excess, the lifetime of the CO shell in most carbon stars will be shorter than that of S Sct. We conclude that double-peaked CO line profiles are very unlikely in carbon stars with a moderate or small 60 μm excess. If they ever would be discovered this would imply a very high mass loss rate in the past.

From Table 2 one can estimate the probability to find a star just after the thermal pulse that turned the star carbon-rich. For some stars (1.5 $M_\odot \lesssim M \lesssim 1.6$ $M_\odot$) this is also the last thermal pulse on the AGB. More massive stars will experience additional thermal pulses. For both the Reimers and the BS mass loss law we find that the probability to observe a carbon star after the thermal pulse that made the star carbon-rich is 45%. Since we argue that the mass loss history of the stars with C/O ratios $\gtrsim$1.5 (a 29% probability) is such that they do not have detached shells this means that at least 63% (45/(100-29)) of the detached shells around optical carbon stars with a 60 μm excess are expected to have oxygen-rich shells.

Acknowledgements. We thank an anonymous referee for constructive comments and for pointing out additional observational material. The research of MG and LBH has been supported under grants 782-373-030 and 782-373-028 by the Netherlands Foundation for Research in Astronomy (ASTRON), which is financially supported by the Netherlands Organisation for Scientific Research (NWO).

References

Aller L.H., Cryzack S.J., 1983, ApJS 51, 211
Aller L.H., Keyes C.D., 1987, ApJS 65, 405
Barbaro G., Dallaporta N., 1974, A&A 33, 21
Barnbaum C., Kastner J.H., Zuckerman B., 1991a, AJ 102, 289
Barnbaum C., Morris M., Likkel L., Kastner J.H., 1991b, A&A 251, 79
Bergeron P., Schaffer R.A., Liebert J., 1992, ApJ 394, 228
Bergman P., Carlström U., Olofsson H., 1993, A&A 268, 685
Blöcker T., Schönberner D., 1993, in: IAU symposium 155 on Planetary Nebulae, eds. R. Weinberger, A. Acker, Reidel, Dordrecht, p. 479 (BS)
Boothroyd A.I., Sackmann I.-J., 1988, ApJ 328, 653
ouchet R., Thé P.S., 1983, PASP 95, 474
Bowen G.H., 1988, ApJ 329, 299
Castellani V., Chieffi A., Straniero O., 1990, ApJS 74, 463
Chan S.J., Kwok S., 1988, ApJ 334, 362
Claussen M.J., Kleinmann S.C., Joyce R.R., Jura M., 1987, ApJS 65, 385
Dean C.A., 1976, AJ 81, 364
de Jong T., 1989, A&A 223, L23
Egan M.P., Leung C.M., 1991, ApJ 383, 314
Eggen O.J., Iben I., 1991, AJ 101, 1377
Engels D., Leinert Ch., 1994, A&A 282, 858
Feast M.W., Glass I.S., Whitelock P.A., Catchpole R.M., 1989, MNRAS 241, 375
Gordon C.P., 1968, PASP 80, 597
Groenewegen M.A.T., de Jong T., van der Bliek N.S., Slijkhuis S., Willems F.J., 1992, A&A 253, 150
Groenewegen M.A.T., 1993, A&A 271, 180
Groenewegen M.A.T., de Jong T., 1993a, A&A 267, 410 (Paper I)
Groenewegen M.A.T., de Jong T., 1993b, A&AS 101, 267
Groenewegen M.A.T., 1994a, A&A submitted
Groenewegen M.A.T., 1994b, A&A in preparation
Groenewegen M.A.T., de Jong T., 1994a, A&A 282, 115
Groenewegen M.A.T., de Jong T., 1994b, A&A 282, 127 (Paper II)
Groenewegen M.A.T., de Jong T., 1994c, A&A 283, 463 (Paper III)
Groenewegen M.A.T., de Jong T., 1994d, A&A in press (Paper IV)
Habing H.J., 1988, A&A 200, 40
Habing H., Tignon J., Tielens A.G.G.M, 1994, A&A 286, 523
Herman J., 1988, A&AS 74, 133
Jørgensen U.G., Westerlund B.E., 1988, A&AS 72, 193
Jorissen A., Mayor M., 1992, A&A 260, 115
Jorissen A., Boffin H., 1992, ESO preprint 832
Jorissen A., Frayer D.T., Johnson H.R., Mayor M., Smith V.V., 1993, A&A 271, 463
Jura M., 1988, ApJS 66, 33
Jura M., Joyce R.R., Kleinmann S.G., 1989, ApJ 336, 924
Jura M., Kleinmann S.G., 1989, ApJ 341, 359
Jura M., Kleinmann S.G., 1992a, ApJS 79, 105
Jura M., Kleinmann S.G., 1992b, ApJS 83, 329
Jura M., Morris M., 1985, ApJ 292, 487
Kaler J.B., Shaw R.A., Kwitter K.A, 1990, ApJ 359, 392
Kastner J.H., Forveille T., Zuckerman B., Omont A., 1993, A&A 275, 163
Kholopov P.N., et al., 1985, General catalog of variable stars, Nauka, Moscow
Lambert D.L., Gustafsson B., Eriksson K., Hinkle K.H., 1986, ApJS 62, 373
Lattanzio J.C., 1991, ApJS 76, 215
Le Bertre T., 1990, A&A 236, 472
Little-Marenin I.R., 1986, ApJ 307, L15
Maeder A., Meynet G., 1989, A&A 210, 155
Mitchell R.M., Robinson G., 1980, MNRAS 190, 669
Morris M., 1975, ApJ 197, 603
Olofsson H., Carlström U., Eriksson K., Gustafsson B., Willson L.A., 1990, A&A 230, L13
Olofsson H., Carlström U., Eriksson K., Gustafsson B., 1992, A&A 253, L17
Olofsson H., Eriksson K., Gustafsson B., Carlström U., 1993, ApJS 87, 267
Olson B.I., Richer H.B., 1975, ApJ 200, 88
Peimbert M., Storey P.J. and Torres-Piembert S., 1993, ApJ 414, 626
Pottasch S.R., 1992, A&AR 4, 215
Reimers D., 1975, in: Problems in stellar atmospheres and envelopes, eds. B. Basheck et al.,Springer, Berlin, p. 229
Reimers D., Grootte D., 1983, A&A 123, 257
Scalo J.M., Miller G.E., 1979, ApJ 233, 596
Schaerer D., Meynet G., Maeder A., Schaller G., 1993, A&AS 98, 523
Schaller G., Schaerer D., Meynet G., Maeder A., 1992, A&AS 96, 269
Schmidt-Kaler Th., 1982, in: Landolt-Bornstein, eds. K. Schaiffers, H.H. Voigt, Springer, Berlin
Schönberner D., 1983, ApJ 272, 708
Smith V.V., Lambert D.L., 1990, ApJS 72, 387
Stephenson C.B., 1989, Publ. Warner and Swasey Obs., Vol. 3, 55
Straižys V., Kuriliene G., 1981, A&SS 80, 353
Sweigart A.V., Greggio L., Renzini A., 1990, ApJ 364, 527
Thronson H.A., Latter W.B., Black J.H., Bally J., Hacking P., 1987, ApJ 322, 770
Tylenda R., Stasinska G., Acker A., Stenholm B., 1991, A&A 246, 221
Tyson N.D., Rich R.M., 1991, ApJ 367, 547
Van den Hoek L.B., Groenewegen M.A.T., Nomoto K., de Jong T., 1994, in preparation
Weidemann V., 1990, ARA&A 28, 103
Whitelock P., et al., 1994, MNRAS 267, 711
Willems F.J., 1988a, A&A 203, 51
Willems F.J., 1988b, A&A 203, 65
Willems F.J., de Jong T., 1986, ApJ 309, L39
Willems F.J., de Jong T., 1988, A&A 196, 173
Wood P.R., Cahn J.H., 1977, ApJ 211, 499
Yamamura I., Onaka T., Kamijo F., Izumiura H., Deguchi S., 1993, PASJ 45, 573
Zijlstra A.A., Loup C., Waters L.B.F.M., de Jong T., 1992, A&A 265, L5
Zuckerman B., Aller L.H., 1986, ApJ 301, 772
Zuckerman B., Maddalena R.J., 1989, A&A 223, L20
Zuckerman B., 1993, A&A 276, 367

This article was processed by the author using Springer-Verlag LaTeX A&A style file version 3.